COBEM 2021 26th International Congress of Mechanical Engineering
November 22-26, 2021, Virtual Congress, Brazil
ABCM Associação Brasileira de Engenharia e Ciências Mecânicas

COB-2021-0680
FLOW-INDUCED VIBRATIONS OF THE DOWNSTREAM CYLINDER IN A TANDEM ARRANGEMENT BASED ON WAKE OSCILLATOR

Rafael Fehér
Juan Pablo Julca Avila
Federal University of ABC - Av. dos Estados, 5001 - Bangú, Santo André - SP, 09210-580. Brazil
rafael_feher@hotmail.com, juan.avila@ufabc.edu.br

Abstract. *When two cylindrical structures are vibrating close to each other, such as risers, power transmission lines and heat exchanger tubes, they experience higher amplitudes of vibration and wider synchronization ranges when compared to the response obtained for a single cylindrical structure. We present a modified wake oscillator model to predict Flow-Induced Vibrations of the downstream cylinder, i.e., the cylinder behind the cylinder exposed to the freestream fluid flow, in a tandem arrangement with two identical smooth rigid cylinders elastically mounted for reduced velocities lower than* 12*. The upstream cylinder was always fixed, while the downstream cylinder was allowed to vibrate. Spacing ratios varying from* 0.3 *to* 3.2 *were simulated and compared with experimental data. For this purpose, an existing vortex-induced vibration model based on a wake oscillator was modified to account for the effects of varying spacing ratios in the downstream cylinder response. Two empirical coefficients were added in the wake oscillator equation and one in the structure oscillator equation of the downstream cylinder to model the wake-induced vibrations generated by the interference between the two cylinders. The model was able to predict the maximum amplitudes of vibration for the downstream cylinder when varying the spacing ratio and results shows to be in good agreement with experimental data.*

Keywords: *Flow Induced Vibrations, Wake Oscillator Model, Fluid-Structure Interaction, Nonlinear Vibrations*

1. INTRODUCTION

When an external fluid flows around bluff structures, such as chimneys, cables that support bridges, antennas, risers etc, an unstable wake is formed behind these structures and the vortices aft them starts to shed. These vortices sheds first from one side of the structure and then from the other side, generating oscillating surface pressures on the structure. If this structure is flexible or flexibly mounted, these oscillating pressures causes the structure to vibrate when the natural frequency of the structure and the frequency of vortex shedding synchronize, in a velocity range known as lock-in. This phenomenon is called Vortex-Induced Vibrations (VIV), that can generate excessive loads on the structure and also fatigue damage. For these reasons, VIV of a single rigid cylinder elastically mounted with one degree of freedom (1-DoF) and two degrees of freedom (2-DoF) still are the subject of many experimental and numerical works through the years. In the experimental field, the main goal is to study the VIV of a single cylinder when varying it's mass, damping and natural frequency, as can be seen in the works of Jauvits and Williamson (2004), Stappenbelt and Lalji (2008) and Blevins and Coughran (2009). The main conclusion of these works, regarding the mass and the damping of the cylinder, is that the maximum amplitude of vibration of the cylinder, defined as $A_y^* = A_y/D$, where A_y is the amplitude of vibration of the cylinder and D is the diameter of the cylinder, tends to increase as the mass ratio and the damping ratio of the cylinder decrease. For mass ratios lower than 6, Jauvits and Williamson (2004) stated that a 2-DoF cylinder reaches amplitudes higher than $1.5D$, where D is the diameter of the cylinder, in an amplitude branch known as the 'super-upper' branch. Moreover, it was found that different results can be obtained for the maximum amplitude of vibration of a cylinder with 1-DoF and of the same cylinder with 2-DoF depending on its mass ratio. In the experiments conducted by Stappenbelt and Lalji (2008), it was seen that for mass ratios lower than 10.63, the maximum amplitudes of vibrations obtained for a cylinder with 1-DoF and 2-DoF are different, with the 2-DoF cylinder reaching higher amplitudes when compared to the 1-DoF cylinder. However, for mass ratios higher than 10.63, both cylinders reache almost the same maximum amplitudes of vibration.

In the numerical field, the main goal is to introduce new mathematical models to predict VIV of cylinders with 1-DoF and 2-DoF elastically mounted. These attempts are commonly made using Computational Fluid Dynamics (CFD), as can be seen in the works of Martins and Avila (2019b), Martins and Avila (2019a) and Khan *et al.* (2018), and using wake oscillator models. The wake oscillator approach consists of using an equation to model the periodic nature of the wake region, commonly a modified van der Pol equation, and an equation to model the motion of the cylinder, commonly the mass-damping-spring equation, with a forcing term on the right-hand side to account for the effects caused by the wake on the cylinder. The goal here is to solve the system of equations for the wake variable, thus satisfying the wake oscillator

equation. Some of these works with 1-DoF and 2-DoF can be found in Skop and Griffin (1973), Facchinetti *et al.* (2004), Srinil and Zanganeh (2012), Kurushina *et al.* (2018), Fehér and Avila (2021) and others. Although providing good results when predicting the VIV of a single rigid cylinder elastically mounted, these models cannot be used to predict Flow Induced Vibrations (FIV) of two cylinders in tandem arrangement.

The study concerning the prediction of FIV of two rigid cylinders elastically mounted in tandem arrangement is of great importance, considering its industrial applications such as inner tubes of heat exchangers, power transmission lines, cables of suspended bridges and others. Unfortunately, such prediction is not easy to achieve, due to the nonlinear and heuristic natures of the phenomenon.

In one of the pioneer works to study this phenomenon, Zdravkovich (1987) categorized various cluster arrangements in terms of the number of cylinders, their mutual spacing and orientation to the freestream fluid flow. He stated that all kinds of interference between two or more cylinders depend strongly on the orientation, spacing and number of cylinders in the cluster. For the case of two parallel cylinders, he distinguished four kinds of flow interference, such as proximity interference, wake interference and a combination of these two interference.

Kim *et al.* (2009) performed a series of 1-DoF experimental analysis for two cylinders in tandem arrangement. They analysed three experimental conditions regarding the cylinders' allowance to vibrate with: (i) both cylinders free to vibrate; (ii) the downstream cylinder free to vibrate with the upstream cylinder fixed; and (iii) the upstream cylinder free to vibrate with the downstream cylinder fixed. Five different regimes of spacing between them were tested and, for each regime, the vibration behaviour of the cylinders was reported. These regimes will be discussed here later.

In the work of Xu *et al.* (2019), a experiment was conducted with two identical elastically mounted circular cylinders in tandem arrangement with 1-DoF. The Reynolds number was between 2.86×10^4–1.14×10^5. Four spacing ratios from 1.57 to 4.57 were tested. They observed that, for the spacing ratio of 4.57 and for a reduced velocity lower than 12.0, the VIV of the cylinders is similar to the one of a single cylinder, whereas the FIV of the upstream cylinder when the spacing ratio is 1.57 is significantly different from that of the isolated cylinder.

The absence of wake oscillator models to predict FIV of two rigid cylinders elastically mounted with 1-DoF for a wide range of spacing ratios was the motivation of this present work. Due to the strongly nonlinear behaviour of the phenomenon, as noticed by Kim *et al.* (2009), we will provide in this work different models to predict the FIV of the downstream cylinder in tandem arrangement, when the upstream cylinder is fixed. Each model will be assigned for one regime of spacing ratio simulated. This will help us to have a more clear view of how the cylinders' interactions changes when varying the spacing between the two cylinders.

The present work is organized as follows: In Section 2. the wake oscillator models used to predict the FIV of the downstream cylinder will be presented. In section 3.the simulation results of the cross-flow reduced amplitude of vibration of the downstream cylinder will be presented. In the final paper, a discussion section will also be presented for observations and final analysis of the results.

2. MODEL DESCRIPTION

Consider two identical circular cylinders with diameters D and mass per unit length m. These cylinders are exposed to a stationary and uniform fluid flow with velocity V and density ρ. Also, the cylinders are separated from each other in a distance T. The upstream cylinder is fixed, while the downstream one is free to vibrate and its motion is described through the coordinated system XY. The downstream cylinder is allowed to vibrate only in the cross-flow direction, defined by the coordinate Y. This cylinder is elastically mounted in the cross-flow direction by springs with stiffness k and linear damping with constants c. The physical model is depicted in Fig. 1.

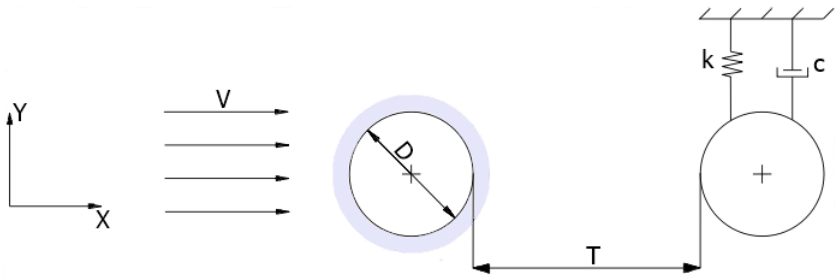

Figure 1: Physical model where the downstream cylinder is free to vibrate while the upstream one is fixed.

2.1 Large regime ($T/D \geq 2.7$)

For this flow regime, experimental data from Kim *et al.* (2009) and Hu *et al.* (2020) shows that the downstream cylinder was almost not affected by the presence of the upstream cylinder when $V_{\mathrm{r}} < 12$, experiencing a vibration similar to pure VIV. With this, and to sustain the FIV analysis as simple as possible in this study, the authors fo this present work

chose to predict the vibration of the downstream cylinder in this regime using a VIV model.

The VIV model used to predict the response of the downstream cylinder in this regime is the one proposed by Facchinetti *et al.* (2004) and it is defined by two equations, the structure oscillator, that models the motion of the cylinder during its oscillations, and the wake oscillator, that models the fluctuating nature of the lift force due to vortex shedding, which are given, respectively, by:

$$\ddot{y} + \left(2\zeta\Omega_{\mathrm{s}} + \frac{\gamma}{m^*}\right)\dot{y} + \Omega_{\mathrm{s}}^2 y = s, \tag{1}$$

$$\ddot{q} + \varepsilon(q^2 - 1)\dot{q} + q = A\ddot{y}, \tag{2}$$

where $y = Y/D$ is the dimensionless displacement of the cylinder in the cross-flow direction, Y in Fig. 1, ζ is the damping ratio and $\Omega_{\mathrm{s}} = \omega_{\mathrm{f}}/\omega_{\mathrm{n}}$ is the frequency ratio of the cylinder, where $\omega_{\mathrm{f}} = 2\pi S_{\mathrm{t}} V/D$ is the vortex-shedding frequency, with St being the Strouhal number and ω_{n} is the natural frequency of the cylinder. γ is the stall parameter, $m^* = m/m_{\mathrm{a}}$ is the mass ratio of the cylinder, where m is the mass per unit length of the cylinder and $m_{\mathrm{a}} = \pi D^2\rho/4$ is the fluid added mass. $s = Mq$ is the forcing term of the structure oscillator, related to the wake variable q, where $M = C_{\mathrm{L0}}/(16\pi^2 S_{\mathrm{t}}^2 m^*)$, with C_{L0} being the lift coefficient measured on a stationary cylinder. ε and A are tuning parameters to fit experimental data and overdots represents derivatives with respect to dimensionless time $\tau = t\omega_{\mathrm{f}}$, where t is the dimensional time.

In the sequel, the variables referring to the upstream cylinder are presented with the subscript "1" and the variables referring to the downstream cylinder with the subscript "2". As the cylinders are identical, with the same damping ratio ζ, the stall parameter γ, the mass ratio m^* and the frequency ratio Ω_{s} are the same for both cylinders, there is no need to use the subscripts in these parameters.

The tuning parameters A and ε in Eq. (2) are used to fit experimental data from a single cylinder experiencing pure VIV when simulating the model composed by Eq. (1) and Eq. (2). Its values are calibrated in Section 3.

2.2 Medium ($0.6 \leq T/D < 2$) and small ($0.2 \leq T/D < 0.6$) regimes

The development of the WIV model begins considering four equations, two of them are the structure oscillator, one for each cylinder, using the same expression of Eq. (1), and the other two are the wake oscillator, also one for each cylinder, using the same expression of Eq. (2). There is no need to use the structure oscillator, Eq. (1), for the upstream cylinder, since this one is fixed and its motion is null, i.e., $y_1 = \dot{y}_1 = \ddot{y}_1 = 0$. This reduces the number of equations to three. Moreover, since $\ddot{y}_1 = 0$, the right-hand side of Eq. (2) is equal to zero for the upstream cylinder, see Eq. (3).

The simplest approach found by the authors of this present work to model the WIV experimented by the downstream cylinder while the upstream one is fixed was to add a new term in the right-hand side of the wake oscillator, Eq. (2), of the downstream cylinder. This term is given by the product of the wake variable of the upstream cylinder, q_1, times a scalar factor, κ, as can be seen in Eq. (5). The experimental data from Kim *et al.* (2009) suggests that the vortex-street of the upstream cylinder is partial development for the medium ($0.6 \leq T/D < 2.0$) and small ($0.2 \leq T/D < 0.6$) regimes of spacing ratios. This is due to the presence of the downstream cylinder in the wake of the upstream one, as can be seen in Fig. 2. This results in a weaker influence of the vortex-shedding from the upstream cylinder in the downstream one, which is modeled by the term κq_1 in Eq. (5).

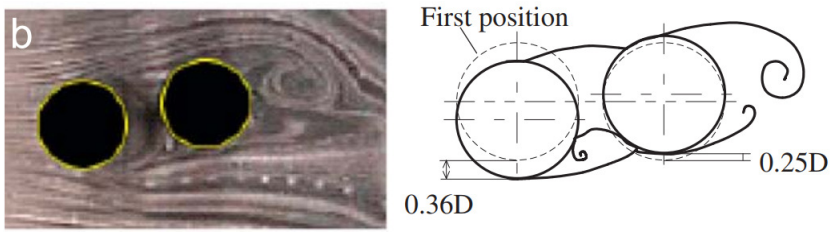

Figure 2: Partial development of the vortex street of the upstream cylinder due to the interference of the downstream one, for $T/D = 0.3$ (Small Regime). Figure extract from the work of Kim *et al.* (2009).

Analyzing the experimental data from Kim *et al.* (2009), it is possible to see that the maximum amplitudes of vibration of the downstream cylinder have its values reduced in about 50% when compared to the results obtained for the same cylinder in the large regime. Also, a delay in the reduced velocity where the lock-in range of the downstream cylinder begins was observed when compared to the results obtained for the large regime.

To account for these differences in the maximum amplitudes of vibration of the downstream cylinder, an empirical parameter, η, is coupled in the right-hand side of the wake oscillator equation of the downstream cylinder, obtaining as final result the Eq. (5). This parameter is multiplying the acceleration coupling term, $A\ddot{y}_2$, and the wake-induced term, κq_1.

It was reported by Xu *et al.* (2019) that the flow velocity experienced by the downstream cylinder differs from the free stream velocity experienced by the upstream cylinder. This difference in the velocities is due to the wake shielding exercised by the upstream cylinder in the wake of the downstream one, resulting in a local reduced velocity. Huang and Herfjord (2013) suggested that this local reduced velocity experienced by the downstream cylinder have influence in its FIV. In fact, one can attribute the delay in the development of the lock-in range to these experimental observations made by Xu *et al.* (2019) and Huang and Herfjord (2013). The simplest approach that we found to account for the delay in the development of the lock-in range of the downstream cylinder, was to modify the structure oscillator of this cylinder, Eq. (1), adding another empirical coefficient, β, alongside the frequency ratio, Ω_s, thus obtaining Eq. (4).

With the correct calibration of the empirical parameters β and η, the same model used to predict the WIV of the downstream cylinder when the upstream cylinder is fixed in the medium regime ($0.6 \leq T/D < 2$) can also be used in the small regime ($0.2 \leq T/D < 0.6$). Such model is given by,

$$\ddot{q}_1 + \varepsilon(q_1^2 - 1)\dot{q}_1 + q_1 = 0, \tag{3}$$

$$\ddot{y}_2 + \left(2\beta\zeta\Omega_\mathrm{s} + \frac{\gamma}{m^*}\right)\dot{y}_2 + \beta\Omega_\mathrm{s}^2 y_2 = s, \tag{4}$$

$$\ddot{q}_2 + \varepsilon(q_2^2 - 1)\dot{q}_2 + q_2 = \eta(A\ddot{y}_2 + \kappa q_1). \tag{5}$$

The two models used in this present work are presented in Tab. 1. This summary will help the readers to have a more clear visualization of each model proposed, depending on the spacing ratio regime and cylinder in question. It is important to point out again that during all the simulations performed in this present work, the upstream cylinder was always fixed while the downstream one was allowed to vibrate in the cross-flow direction.

Table 1: Mathematical models to predict FIV of the downstream cylinder depending on the spacing ratio.[(1)]

Spacing Ratios	**Downstream Cylinder FIV Models**	**Parameters**
Small Regime ($0.2 \leq T/D < 0.6$) **and Medium Regime** ($0.6 \leq T/D < 2$)	**Wake-induced vibration:** $\ddot{q}_1 + \varepsilon(q_1^2 - 1)\dot{q}_1 + q_1 = 0,$ $\ddot{y}_2 + \left(2\beta\zeta\Omega_\mathrm{s} + \frac{\gamma}{m^*}\right)\dot{y}_2 + \beta\Omega_\mathrm{s}^2 y_2 = s,$ $\ddot{q}_2 + \varepsilon(q_2^2 - 1)\dot{q}_2 + q_2 = \eta(A\ddot{y}_2 + \kappa q_1).$	q_1: Wake variable of the upstream cylinder; q_2: Wake variable of the downstream cylinder; y_2: Cross-flow displacement of the cylinder; ζ, m^*, Ω_s: Damping, mass and frequency ratios; β, η, κ: WIV empirical coefficients.
Large Regime ($T/D \geq 2.7$)	**Vortex-induced vibration:** $\ddot{y}_2 + \left(2\zeta\Omega_\mathrm{s} + \frac{\gamma}{m^*}\right)\dot{y}_2 + \Omega_\mathrm{s}^2 y_2 = s,$ $\ddot{q}_2 + \varepsilon(q_2^2 - 1)\dot{q}_2 + q_2 = A\ddot{y}_2.$	

[(1)] According to Kim *et al.* (2009), the downstream cylinder does not vibrate for $0.1 \leq T/D < 0.2$ and $2.0 \leq T/D < 2.7$.

3. RESULTS

The parameters used in all simulations conducted in this work are presented in Tab. 2.

Table 2: Simulation parameters.

Parameter	Kim *et al.* (2009)	Hu *et al.* (2020)	Unit
Diameter of the cylinders, D	0.066	0.066[(2)]	m
Natural frequency of the cylinders in still fluid, ω_s	62.83	9.36	rad/s
Mass ratio of the cylinders, m^*	110	320	-
Damping ratio of the cylinders, ζ	0.002	0.0009	-
Lift coefficient measured on the stationary cylinder, C_L0	0.3	0.3	-
Strouhal number, S_t	0.2	0.2	-
Stall parameter, γ[(3)]	0.8	0.8	-

[(2)] Hu *et al.* (2020) does not provided the value of D. Thus, the same D used by Kim *et al.* (2009) was used.

[(3)] The stall parameter is actually a hydrodynamic parameter to simulate the model and does not depend on the experimental parameters. Therefore, the same value used by Facchinetti *et al.* (2002) was used.

3.1 Large regime ($T/D > 2.7$)

For this regime, the experimental data from Kim *et al.* (2009) shows that the vibration of the downstream cylinder was almost not affected by the presence of the upstream cylinder when $V_\mathrm{r} < 14$, hence, we chose to use the VIV model to

predict the vibration of the downstream cylinder in this regime. The curve of cross-flow reduced amplitude vs. reduced velocity presented in Fig. 3 was obtained by simulating the VIV model from Tab. 1, Eq. (1) and Eq. (2). A simulation using the experimental data from Hu *et al.* (2020), presented in Tab. 2, was made to illustrate the difference in the maximum amplitude of vibration for cylinders with different mass-damping parameter, $m^*\zeta$.

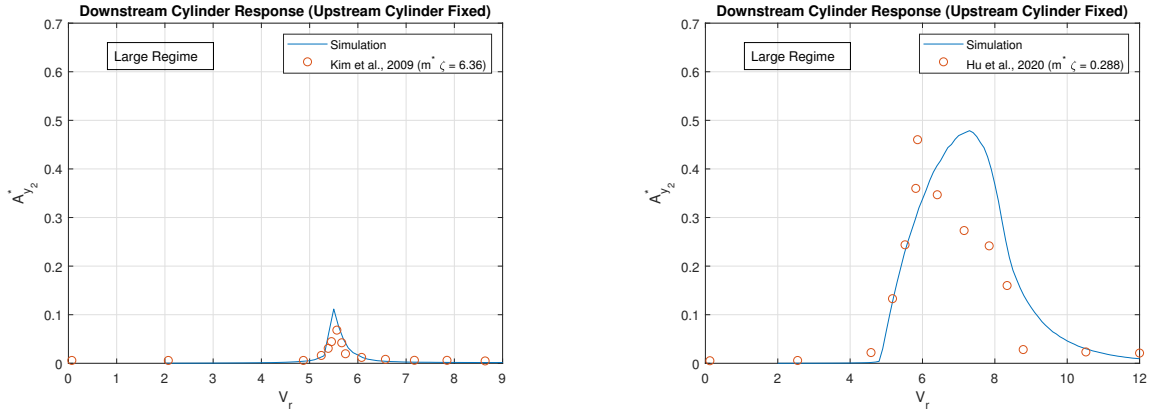

(a) Comparison with Kim *et al.* (2009): $m^*\zeta = 6.36$ (b) Comparison with Hu *et al.* (2020): $m^*\zeta = 0.288$

Figure 3: Curve of cross-flow reduced amplitude vs. reduced velocity obtained using the VIV model from Tab. 1, Eq. (1) and Eq. (2), when the downstream cylinder is allowed to vibrate while the upstream one is fixed, for large regime. Comparison with experimental data from: (a) Kim *et al.* (2009) ($T/D = 3.2$), and (b) Hu *et al.* (2020) ($T/D = 3.0$).

Fig. 3 shows the difference in the maximum amplitude of vibration of the cylinder when varying the mass-damping parameter, $m^*\zeta$. For a higher value of $m^*\zeta = 6.36$, Fig. 3a, one can see a smaller maximum amplitude of vibration of $A^*_{y_2} \cong 0.11$ when compared to the maximum amplitude of vibration of $A^*_{y_2} \cong 0.48$, obtained for $m^*\zeta = 0.288$, Fig. 3b. This was experimentally observed by Jauvits and Williamson (2004) and Stappenbelt and Lalji (2008), in which the maximum amplitudes of vibration of the cylinder decreases with the mass ratio.

In terms of tuning parameter calibration, this implies that the parameter A in Eq. (2) has to assume lower values as $m^*\zeta$ decreases, while the parameter ε has to assume higher values. This calibration process was made by Fehér and Avila (in-press) for different mass and damping ratios and the same trend was observed. Therefore, to generate the curve presented in Fig. 3a, for $m^*\zeta = 6.36$, the tuning parameters (2) were set to: $A = 0.5$ and $\varepsilon = 0.8$, and to generate the curve presented in Fig. 3b, for $m^*\zeta = 0.288$, the tuning parameters (2) were set to: $A = 10.5$ and $\varepsilon = 0.3$. For a better visualization, these parameters are presented in Tab. 3.

Table 3: Tuning parameters to generate the curves in Fig. 3.

$\boldsymbol{m^*\zeta = 6.36}$	$\boldsymbol{m^*\zeta = 0.288}$
$A = 0.5$	$A = 10.5$
$\varepsilon = 0.8$	$\varepsilon = 0.3$

One can obtain the same response presented in Fig. 3 using the WIV model, Eq. (3)-(5), with $\beta = 1$, $\eta = 1$ and $\kappa = 0$. Although, the VIV model, Eq. (1) and Eq. (2), have less empirical coefficients and equations, leading to a less time-consuming simulation.

3.2 Medium regime ($0.6 \leq T/D < 2$)

The results obtained when simulating the model for $T/D = 1.1$ and $T/D = 1.2$ (Medium Regime) are presented in Fig. 4. This curves are generated by simulate the WIV model, composed by Eqs. (3)-(5), as can be seen in Tab. 1.

One can see in Fig. 4 that the model was able to predict the maximum amplitudes of vibration for both cases: $A^*_{y_2} \cong 0.15$, reported by Kim *et al.* (2009), and $A^*_{y_2} \cong 0.50$, reported by Hu *et al.* (2020). Also, tuning the delay lock-in coefficient, β, the model was able to predict the reduced velocity where the lock-in range begins, at $V_r \cong 6.0$, for Kim *et al.* (2009), and $V_r \cong 3.45$, for Hu *et al.* (2020).

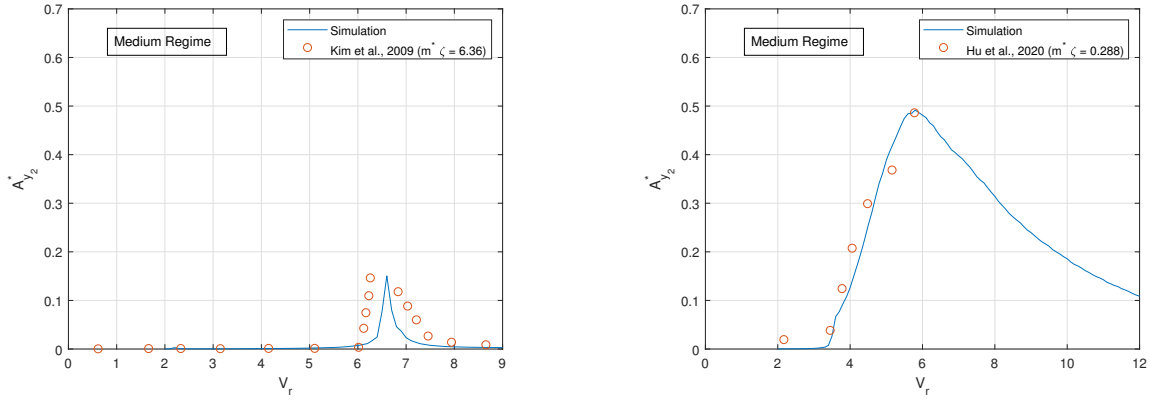

(a) Comparison with Kim *et al.* (2009): $m^*\zeta = 6.36$ (b) Comparison with Hu *et al.* (2020): $m^*\zeta = 0.288$

Figure 4: Curve of cross-flow reduced amplitude vs. reduced velocity obtained using the WIV model from Tab. 1, Eqs. (3)-(5), when the downstream cylinder is allowed to vibrate while the upstream one is fixed, for medium regime. Comparison with experimental data from: (a) Kim *et al.* (2009) ($T/D = 1.2$), and (b) Hu *et al.* (2020) ($T/D = 1.1$).

Again, the difference in the maximum amplitude of vibration observed when comparing Fig. 4a and Fig. 4b is due to the different values of $m^*\zeta$ used by these authors. This higher value was expected, since a lower value of $m^*\zeta$ results in higher amplitudes of vibration, as observed by Jauvits and Williamson (2004). This shows how complex is the development of a comprehensive wake oscillator model to predict the FIV of two cylinders in tandem arrangement, considering different parametric behaviors, particularly when changing $m^*\zeta$ and the spacing ratio. Again the same trend is observed, with the higher $m^*\zeta = 6.36$ resulting in lower $A^*_{y_2}$.

The empirical coefficients used in the WIV model for each case of $m^*\zeta$ are presented in Tab. 3. Remembering that the parameters A and ε are fixed at the values obtained in the Large Regime, namely $A = 0.5$ and $\varepsilon = 0.8$, for $m^* = 6.36$, and $A = 10.5$ and $\varepsilon = 0.3$, for $m^* = 0.288$.

Table 4: Empirical coefficients to generate the curves in Fig. 4.

$\boldsymbol{m^*\zeta = 6.36}$	$\boldsymbol{m^*\zeta = 0.288}$
$\beta = 1.6$	$\beta = 0.5$
$\eta = 2.0$	$\eta = 1.065$
$\kappa = 0.5$	$\kappa = 0.5$

One interesting observation is that, in Fig. 4b, it can be seen that there is no delay in the development of the lock-in range, in fact, it start to develop earlier, at $V_\mathrm{r} \cong 3.45$ when compared to Fig. 4a, at $V_\mathrm{r} \cong 6.0$. This probably occurs due to the difference in $m^*\zeta$ and natural frequencies of the cylinders in each experiment, since the spacing between cylinders is almost the same for both cases, with $T/D = 1.2$ for Kim *et al.* (2009) and $T/D = 1.1$ for Kim *et al.* (2009).

With the spacing between the two cylinders being almost the same for both cases, there is no need to use different values of κ parameter, and for this reason, κ have the same value in both columns of Tab. 4. Moreover, this parameter assumes lower values as T/D decreases, since it is responsible to model the partial development of the vortex-shedding of the upstream cylinder due to the presence of the downstream one, see Fig. 2.

As the initial velocities where the development of lock-in range begins are different for each experiment, β has different values in Tab. 4. For a higher V_r where the development of lock-in range begins, in Kim *et al.* (2009) at $V_\mathrm{r} \cong 6.0$, $\beta = 1.6$ and, For a lower V_r where the development of lock-in range begins, in Hu *et al.* (2020) at $V_\mathrm{r} \cong 3.45$, $\beta = 0.5$. Observe that the value of β increases with V_r.

There is no comparison between the η parameter calibrated for each simulation, since its value depends on A and ε, which are different for Kim *et al.* (2009) and for Hu *et al.* (2020), see Tab. 3.

3.3 Small regime $(0.2 \leq T/D < 0.6)$

To predict the FIV of the downstream cylinder for this regime, the WIV model presented in Tab. 1, Eqs. (3)- (5), was used.

The results obtained are presented in Fig. 5. It is possible to see that the maximum amplitude of vibration of the downstream cylinder predicted by the model was $A^*_{y_2} \cong 0.091$ at $V_\mathrm{r} \cong 5.7$. This value is slightly higher than the one from experimental data, where $A^*_{y_2} \cong 0.08$ at $V_\mathrm{r} \cong 6.0$, with an error of prediction of 16.6% when compared to the response measured by Kim *et al.* (2009). Considering that for this range of gap ratios the maximum amplitude of vibration is in

the order of $0.1D$, an error of 16.6% corresponds to approximately $0.016D$ in the maximum value of cross-flow reduced amplitude of the cylinder, therefore, this difference was neglected in this analysis.

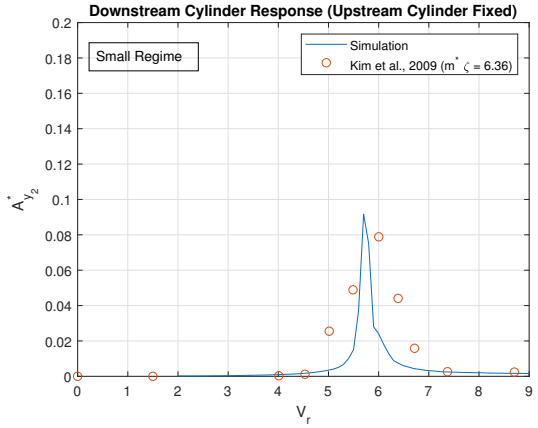

Figure 5: Curve of cross-flow reduced amplitude vs. reduced velocity obtained using the wake oscillator model from Tab. 1, Eqs. (3)- (5), when the downstream cylinder is allowed to vibrate while the upstream one is fixed, for $T/D = 0.3$. Experimental data from Kim *et al.* (2009), represented by '$\circ$'.

As was mentioned in Section 2.κ is responsible to tune the influence of q_1 in the motion of the downstream cylinder. Since for the small regime of spacing ratios the wake of the upstream cylinder is partial developed due to the presence of the downstream cylinder, see Fig. 2, a low value of $\kappa = 0.001$ was needed to be set in Eq. (5) to match experimental data.

The β parameter was added in the structure oscillator of the downstream cylinder, Eq. (4), to model the delay in the beginning of the development of lock-in. For the results presented in Fig. 5, $\beta = 1.2$ in Eq. (4), which forces the initial development of the lock-in range to occur at higher reduced velocities.

Finally, the parameter η in the right-hand side of Eq. (5) acts as a scalar factor for the whole forcing-term, $(A\ddot{y}_2 + \kappa q_1)$, i.e., higher values of η results in higher values of $A^*_{y_2}$. For the results presented in Fig. 5, $eta = 0.1$. Therefore, the values of the empirical coefficients used to generate the curve presented in Fig. 5 were: $\beta = 1.2$, $\eta = 0.1$ and $\kappa = 0.001$, as can be seen in Tab. 5.

Table 5: Empirical coefficients to generate the curves in Fig. 5.

$\boldsymbol{m^*\zeta = 6.36}$
$\beta = 1.2$
$\eta = 0.1$
$\kappa = 0.001$

An analysis can be conducted regarding the different maximum amplitudes of vibration, $A^*_{y_{2\text{max}}}$, obtained when varying T/D with the same $m^*\zeta$, and vice-versa. These results are presented in Fig. 6.

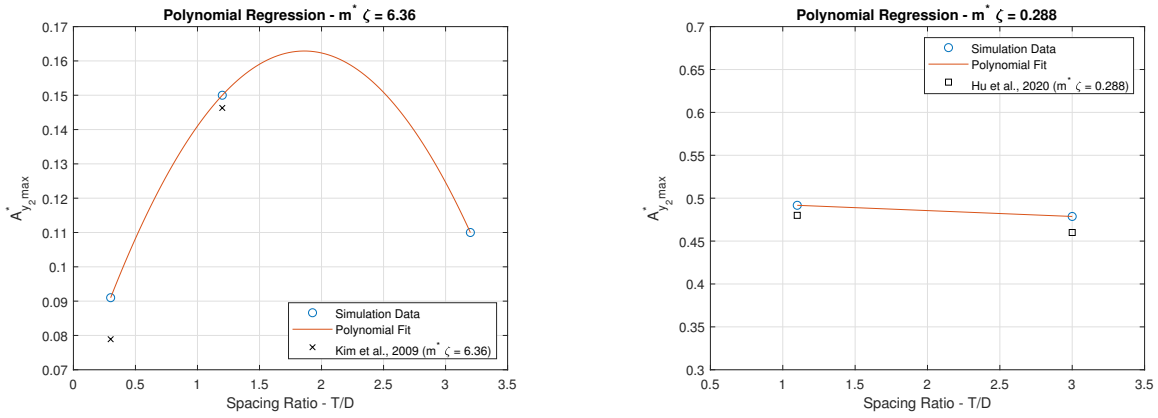

(a) $m^*\zeta = 6.36$ (b) $m^*\zeta = 0.288$

Figure 6: Maximum values of cross-flow reduced amplitude when varying spacing ratio. Experimental data from: (a) Kim *et al.* (2009), for $m^*\zeta = 6.36$, represented by $\times$ and (b) Hu *et al.* (2020), for $m^*\zeta = 2.36$, represented by $\square$.

Observing Fig. 6, one can see that the maximum amplitudes of vibration, $A^*_{y_{2\max}}$, has lower values for the cases where $m^*\zeta = 6.36$, Fig. 6a, when compared to the values in Fig. 6b, where $m^*\zeta = 0.288$. Thus, higher maximum amplitudes of vibration are found for a lower $m^*\zeta$. Moreover, these differences may also be related to other experimental parameters, such as the natural frequency of the cylinder, that has different values in the experiments conducted by Kim *et al.* (2009) when compared to Hu *et al.* (2020).

The equations of the polynomial fit observed in Fig. 6 for each $m^*\zeta$ are presented in Tab. 6:

Table 6: Equations to predict the maximum amplitudes of vibration presented in Fig. 6 for different $m^*\zeta$ as function of T/D.

$m^*\zeta$	Equation
6.36	$A^*_{y_{2\max}} \cong -0.0295(T/D)^2 + 0.11(T/D) + 0.06$
0.288	$A^*_{y_{2\max}} \cong -0.007(T/D) + 0.50$

It is important to remember that these equations are only valid for $0.3 \leq T/D \leq 3.5$ and for $m^*\zeta = 6.36$ (first line of Tab. 6) and $m^*\zeta = 0.288$ (second line of Tab. 6). Although they can be used to give an estimation of $A^*_{y_{2\max}}$. For instance, with $m^*\zeta = 3.36$, one can expect the same trend in $A^*_{y_{2\max}}$ as observed in Fig. 6a, but with higher values, as $m^*\zeta$ is lower when compared to $m^*\zeta = 6.36$.

A similar analysis can be conducted regarding the different values of empirical coefficients, β, η and κ, used for each case of $m^*\zeta$ during simulations using the WIV model, Eqs. (3)-(5) when varying spacing ratio. These results are presented in Tab. 4 (for Medium Regime) and in Tab. 5 (for Small Regime), remembering that the parameters A and ε are fixed at the values obtained for the Large Regime, namely $A = 0.5$ and $\varepsilon = 0.8$, for $m^* = 6.36$, and $A = 10.5$ and $\varepsilon = 0.3$, for $m^* = 0.288$. Fig. 7 presents the empirical coefficients used for $m^*\zeta = 6.36$.

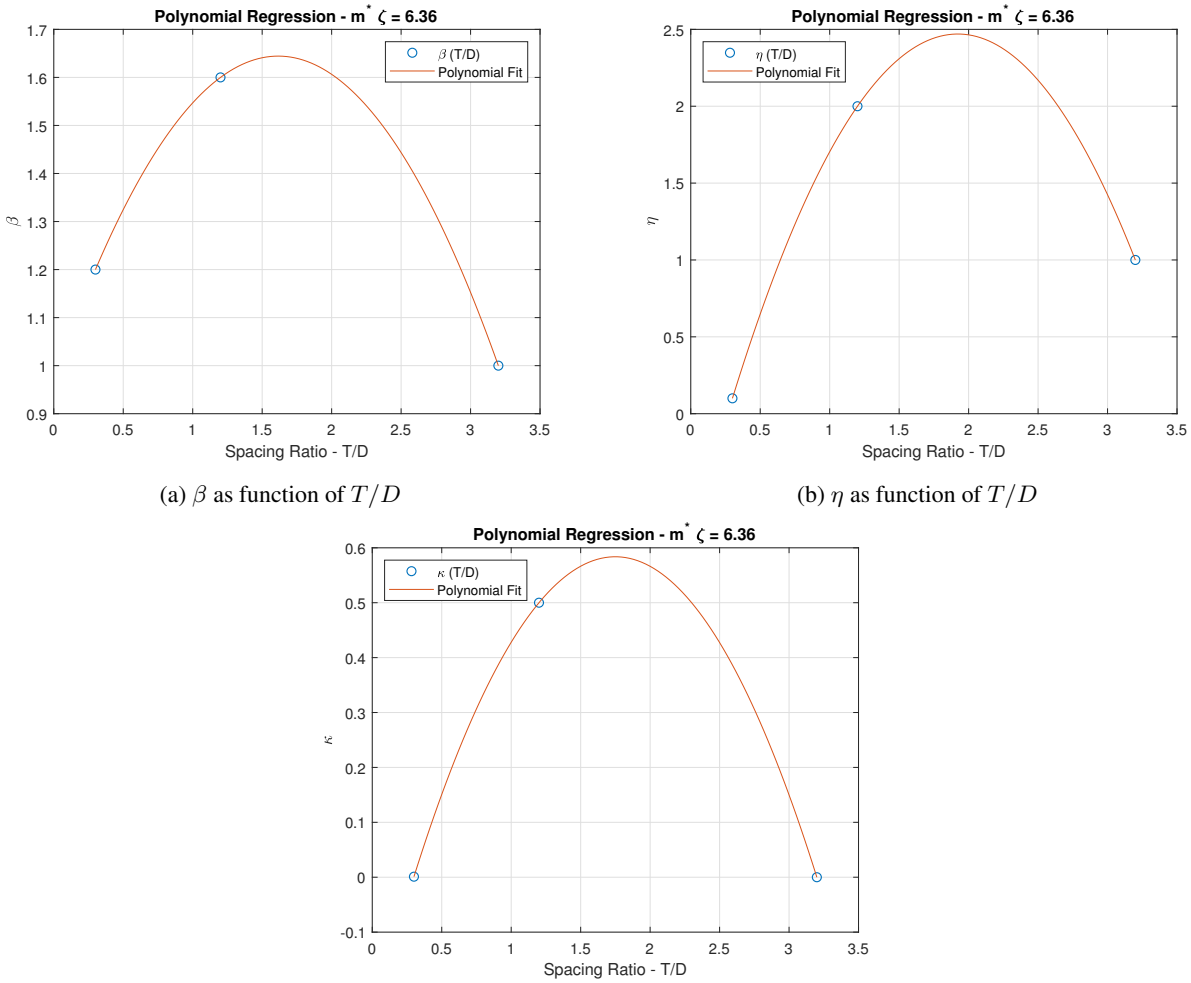

(a) β as function of T/D

(b) η as function of T/D

(c) κ as function of T/D

Figure 7: Empirical coefficients used to simulate the WIV model for $m^*\zeta = 6.36$ and $0.3 \leq T/D \leq 3.2$.

And its respective equations are:

Table 7: Equations to predict the empirical coefficients presented in Fig. 7 for $m^*\zeta = 6.36$ as function of T/D.

Empirical Coef.	**Equation**
$\boldsymbol{\beta}$	$\beta \cong -0.256(T/D)^2 + 0.830(T/D) + 0.974$
$\boldsymbol{\eta}$	$\eta \cong -0.9(T/D)^2 + 3.461(T/D) - 0.857$
$\boldsymbol{\kappa}$	$\kappa \cong -0.277(T/D)^2 + 0.970(T/D) - 0.265$

4. DISCUSSION

This work had as main goal to propose a new model based on wake oscillator to predict the WIV of the downstream cylinder in a tandem arrangement for $T/D < 3.2$ while the upstream cylinder was fixed. Most of the experimental works found by the authors of this work was based on explore the FIV of two cylinders in tandem arrangement for $T/D > 3.0$, with little effort made to study the FIV of these cylinders for spacing ratios lower than 3.0. Moreover, no works were found based on wake oscillators to predict the FIV of two cylinders in tandem arrangement with $T/D < 3.0$ based on wake oscillators, and it is here that the present work have its most valuable contribution.

A new model based on wake oscillator was proposed to predict the FIV of the downstream cylinder in a tandem arrangement for spacing ratios between $0.3 \leq T/D \leq 3.2$ and $V_{\text{r}} < 12$. Based on comparisons with experimental data, the following remarks can be drawn.

(1) The model was able to capture two main features of FIV (the maximum amplitudes of vibration and the lock-in range) of the downstream cylinder depicted in Fig. 1, for all spacing ratios and $m^*\zeta$ simulated.

(2) Coupling new empirical coefficients to the wake oscillator model to predict the WIV of the downstream cylinder while the upstream one was fixed, i.e., β in Eq. (4), η and κ in Eq. (5), one can control the position of the lock-in range, the amplitude of vibration of the downstream cylinder depending on T/D and how much the wake of the upstream cylinder influences the downstream one. With these empirical coefficients, one can predict the FIV of the downstream cylinder for different conditions of T/D, and mass-damping parameters. Also, one can use the WIV model composed by Eq. (3) to Eq. (5) to predict the VIV of a single cylinder. To do so, one simply needs to adjust $\beta = \eta = 1$ and $\kappa = 0$, which indicates the level of flexibility of the models proposed.

(4) After these calibration with experimental data, equations were generated to calculate each empirical coefficient as function of T/D for $m^*\zeta = 6.36$ and $m^*\zeta = 0.288$

(5) After the simulations, equations where generated to predict the maximum amplitudes of vibration, $A^*_{y_{2\text{max}}}$, as function of T/D for $m^*\zeta = 6.36$ and $m^*\zeta = 0.288$

(6) The model was not able to predict the wake-galloping vibration that occurs for $V_{\text{r}} > 12$, that can be seen in the works of Xu *et al.* (2019) and Hu *et al.* (2020). This FIV would only be possible to predicted with a more complex WIV model, that could predict both wake-induced and wake-galloping vibrations. In fact, this is the subject of a future research, and we believe that, even with no wake-galloping prediction the models proposed here will enrich the state-of-art of the subject.

5. ACKNOWLEDGEMENTS

Rafael Fehér wishes to acknowledge support given to him from Federal University of ABC through scholarship during all the research period.

6. REFERENCES

Blevins, R.D. and Coughran, C.S., 2009. "Experimental Investigation of Vortex-Induced Vibration in One and Two Dimensions With Variable Mass, Damping, and Reynolds Number". *Journal of Fluids Engineering*, Vol. 131, No. 10.

Facchinetti, M.L., [de Langre], E. and Biolley, F., 2004. "Coupling of structure and wake oscillators in vortex-induced vibrations". *Journal of Fluids and Structures*, Vol. 19, No. 2, pp. 123 – 140. ISSN 0889-9746. doi:https://doi.org/10.1016/j.jfluidstructs.2003.12.004. URL `http://www.sciencedirect.com/science/article/pii/S0889974603001853`.

Facchinetti, M., de Langre, E., Fontaine, E., Bonnet, P., Etienne, S. and Biolley, F., 2002. "Viv of two cylinders in tandem arrangement: Analytical and numerical modeling". Vol. 12.

Fehér, R. and Avila, J.J., 2021. "Vortex-induced vibrations model with 2 degrees of freedom of rigid cylinders near a plane boundary based on wake oscillator". *Ocean Engineering*, Vol. 234, p. 108938. ISSN 0029-8018. doi:https://doi.org/10.1016/j.oceaneng.2021.108938. URL `https://www.sciencedirect.com/science/article/pii/S0029801821003735`.

Fehér, R. and Avila(in-press), J.J., 2021. "Parametric behaviour of a vortex-induced vibration model of cylinders with 2 degrees of freedom using a wake oscillator". *Journal of Offshore Mechanics and Arctic Engineering*. In-press.

Hu, Z., Wang, J. and Sun, Y., 2020. "Cross-flow vibrations of two identical elastically mounted cylinders in tandem arrangement using wind tunnel experiment". *Ocean Engineering*, Vol. 209, p. 107501. ISSN 0029-8018. doi:https://doi.org/10.1016/j.oceaneng.2020.107501. URL https://www.sciencedirect.com/science/article/pii/S002980182030514X.

Huang, S. and Herfjord, K., 2013. "Experimental investigation of the forces and motion responses of two interfering viv circular cylinders at various tandem and staggered positions". *Applied Ocean Research*, Vol. 43, pp. 264–273. ISSN 0141-1187. doi:https://doi.org/10.1016/j.apor.2013.10.003. URL https://www.sciencedirect.com/science/article/pii/S0141118713000801.

Jauvits, N. and Williamson, C.H.K., 2004. "The effect of two degrees of freedom on vortex-induced vibration at low mass and damping". *Journal of Fluid Mechanics*, Vol. 509, p. 23–62. doi:10.1017/S0022112004008778.

Khan, N.B., Ibrahim, Z., Khan, M.I., Hayat, T. and Javed, M.F., 2018. "Viv study of an elastically mounted cylinder having low mass-damping ratio using rans model". *International Journal of Heat and Mass Transfer*, Vol. 121, pp. 309 – 314. doi:https://doi.org/10.1016/j.ijheatmasstransfer.2017.12.109.

Kim, S., Alam, M.M., Sakamoto, H. and Zhou, Y., 2009. "Flow-induced vibrations of two circular cylinders in tandem arrangement. part 1: Characteristics of vibration". *Journal of Wind Engineering and Industrial Aerodynamics*, Vol. 97, No. 5, pp. 304–311. ISSN 0167-6105. doi:https://doi.org/10.1016/j.jweia.2009.07.004. URL https://www.sciencedirect.com/science/article/pii/S0167610509000579.

Kurushina, V., Pavlovskaia, E., Postnikov, A. and Wiercigroch, M., 2018. "Calibration and comparison of viv wake oscillator models for low mass ratio structures". *International Journal of Mechanical Sciences*, Vol. 142. doi:10.1016/j.ijmecsci.2018.04.027.

Martins, F.A.C. and Avila, J.P.J., 2019a. "Effects of the reynolds number and structural damping on vortex-induced vibrations of elastically-mounted rigid cylinder". *International Journal of Mechanical Sciences*, Vol. 156, pp. 235 – 249. ISSN 0020-7403. doi:https://doi.org/10.1016/j.ijmecsci.2019.03.024. URL http://www.sciencedirect.com/science/article/pii/S0020740318343133.

Martins, F.A.C. and Avila, J.P.J., 2019b. "Three-dimensional cfd analysis of damping effects on vortex-induced vibrations of 2dof elastically-mounted circular cylinders". *Marine Structures*, Vol. 65, pp. 12 – 31. ISSN 0951-8339. doi:https://doi.org/10.1016/j.marstruc.2019.01.005. URL http://www.sciencedirect.com/science/article/pii/S0951833918302880.

Skop, R. and Griffin, O., 1973. "A model for the vortex-excited resonant response of bluff cylinders". *Journal of Sound and Vibration*, Vol. 27, No. 2, pp. 225–233. ISSN 0022-460X. doi:https://doi.org/10.1016/0022-460X(73)90063-1.

Srinil, N. and Zanganeh, H., 2012. "Modelling of coupled cross-flow/in-line vortex-induced vibrations using double duffing and van der pol oscillators". *Ocean Engineering*, Vol. 53, pp. 83–97. doi:10.1016/j.oceaneng.2012.06.025.

Stappenbelt, B. and Lalji, F., 2008. "Vortex-induced vibration super-upper response branch boundaries". *International Journal of Offshore and Polar Engineering*, Vol. 18.

Xu, W., Ji, C., Sun, H., Ding, W. and Bernitsas, M.M., 2019. "Flow-induced vibration of two elastically mounted tandem cylinders in cross-flow at subcritical reynolds numbers". *Ocean Engineering*, Vol. 173, pp. 375–387. ISSN 0029-8018. doi:https://doi.org/10.1016/j.oceaneng.2019.01.016. URL https://www.sciencedirect.com/science/article/pii/S0029801819300174.

Zdravkovich, M., 1987. "The effects of interference between circular cylinders in cross flow††an earlier version as originally presented as an invited paper, entitled "forces on pipe clusters", at the international symposium on separated flow around marine structures, norwegian institute of technology, trondheim, norway, 26–28 june 1985." *Journal of Fluids and Structures*, Vol. 1, No. 2, pp. 239–261. ISSN 0889-9746. doi:https://doi.org/10.1016/S0889-9746(87)90355-0. URL https://www.sciencedirect.com/science/article/pii/S0889974687903550.

7. RESPONSIBILITY NOTICE

The authors are solely responsible for the printed material included in this paper.